Korean J. Chem. Eng., 33(4), 1500-1504 (2016)
DOI: 10.1007/s11814-015-0274-9

pISSN: 0256-1115
eISSN: 1975-7220

A facile synthetic route for Co_3O_4 nanoparticle/porous carbon composite as an efficient anode material for lithium-ion batteries

Nulu Venugopal[**], **Woo-Sik Kim**[*], **and Taekyung Yu**[*,†]

*Department of Chemical Engineering, Kyung Hee University, Yongin 17104, Korea
**Department of Energy Science, Sungkyunkwan University, Suwon 440-746, Korea
(*Received 4 August 2015 • accepted 8 December 2015*)

Abstract−Facile synthesis and electrochemical performance of a Co_3O_4 nanoparticles/porous carbon composite used as an anode in Li-ion batteries is reported in this work. Co_3O_4 nanoparticles (5-10 nm in size) were embedded in a disordered porous carbon network using a simple template-free chemical method. The synthesized composite work well as an anode material for Li-ion batteries by delivering stable cycle life and highly reversible capacities of 480 $mAhg^{-1}$ at 500 mAg^{-1}, which is higher than that of commercially available graphite electrodes and is comparable to values reported for Co_3O_4/graphene composites.

Keywords: Co_3O_4, Porous Carbon, Nanoparticles, Anode Materials, Composite Material

INTRODUCTION

Nanoscale transition metal oxides (NiO, CoO, FeO, CuO, Cu_2O, and Co_3O_4) have been investigated as anode materials for lithium-ion batteries (LIBs) due to their higher reversible capacities compared with conventional graphite anode materials [1]. Researchers have increasingly focused on MO_x (M=transition metal) composites made with a variety of carbon materials as alternative anode materials for LIBs [2-6]. Among the transitional metal oxides, Co_3O_4 has attracted much attention because its precursors are commercially available and it has a high specific theoretical capacity. However, Co_3O_4 often suffers from large volume expansion and poor cycle life. To circumvent these problems, researchers have pursued a promising strategy to construct hybrid materials including mixed metal oxide/carbon nanotubes [**7**], nanoscale carbon/Co_3O_4 [8], Co_3O_4/carbon nanotubes [9], and Co_3O_4/reduced graphene oxide [10]. All these composite materials meet the desired requirements of anode materials in LIBs by providing stable cycle life and good rate capability. However, the synthesis methods employed to obtain hybrid materials involve complicated steps such as high-temperature inert atmosphere carbonization, which is required to obtain crystalline CoO_x particle/carbon composites. Therefore, a suitable facile alternative method to obtain Co_3O_4/carbon composite materials is required. Furthermore, the use of porous carbon can enhance the resulting anode electrode performance [7]. We employed Super-P carbon black (carbon nanoparticles) as the carbonization precursor for Co_3O_4/C composite preparation.

†To whom correspondence should be addressed.
E-mail: tkyu@khu.ac.kr

EXPERIMENTAL

The Co_3O_4 nanoparticles/porous carbon composite (Co_3O_4/C) was prepared by a modified chemical method [11]. In a typical synthesis, 0.9 g $Co_2(CO)_8$ (99.999%, Sigma Aldrich) and 0.32 g of Super-P carbon black (carbon nanoparticles, ~50 nm) were added to 100 ml of hexane under an inert atmosphere in an argon-filled glove box. The resulting mixture was sonicated in an open atmosphere for 10 min at room temperature. The resulting solid product was separated by centrifugation and washed with distilled water and ethanol. The solid was oven dried at 100 °C for 1 h followed by annealing at 300 °C for 1 h in air (hereafter, this is referred to as sample CC). For comparison, a bare Co_3O_4 powder was prepared by the same method without adding Super-P carbon black (i.e., sample C).

The samples were characterized using X-ray diffraction (XRD, Rigaku, Rint-2000 using Cu-Kα radiation), field emission scanning electron microscopy (FE-SEM, Hitachi, S-4800), transmission electron microscopy (TEM, JEOL JEM 2010, 200 kV), and thermogravimetric analysis (TGA, NETZSCH TG 209 T3 Taurus).

Electrodes for lithium ion batteries were prepared by mixing 90 wt% Co_3O_4/C and 10 wt% polyvinylidene fluoride (PVDF, 6 wt%) in an N-methyl-2-pyrrolidinone (NMP) solution to make a slurry. The prepared slurry was uniformly spread onto a Cu foil. The electrodes were dried at 100 °C for 1 h, roll pressed, and dried again in a vacuum oven at 90 °C for 3 h. For comparison, a bare Co_3O_4 electrode was prepared with weight ratios of 80:10:10 (Co_3O_4 : Super-P : PVDF). Electrochemical tests were performed with 2032 coin-type cells. The mass loading was ~1.1 mg cm^{-2} for both the electrodes. The electrolyte solution was 1.2 M $LiPF_6$ in a solvent that was a mixture of ethylene carbonate (EC) and ethyl methyl carbonate (EMC) at a 3 : 7 ratio by volume. The cells were assembled in

an argon-filled glove box. Galvanostatic charge-discharge tests were carried out with a battery tester (TOSCAT-3100U) in the potential range of 0.01-3 V *vs.* Li^+/Li at a temperature of 25 °C.

RESULTS AND DISCUSSION

1. Material Characterization

Fig. 1 shows the XRD patterns of the Co_3O_4 (Fig. 1(a)(i)) and the composite Co_3O_4/C (Fig. 1(a)(ii)). For sample C, the diffraction patterns matched well with those of the reference patterns for spinel Co_3O_4 (JCPDS 42-1467). The XRD pattern of the composite shows the well-aligned peaks of Co_3O_4. The small carbon peak at 2θ= 25° in Fig. 1(a)(ii) indicates the successful formation of a composite of Co_3O_4 and graphitic carbon.

To determine the carbon content in the composite, thermal oxidation of Super-P carbon, Co_3O_4, and hybrid Co_3O_4/C was studied

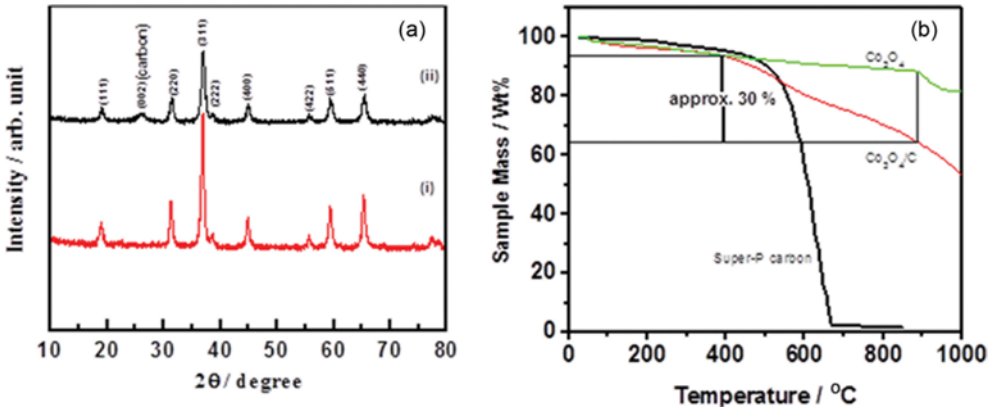

Fig. 1. (a) XRD patterns of (i) Co_3O_4 and (ii) Co_3O_4/C. (b) TGA curves of Super-P carbon, Co_3O_4 and Co_3O_4/C composite.

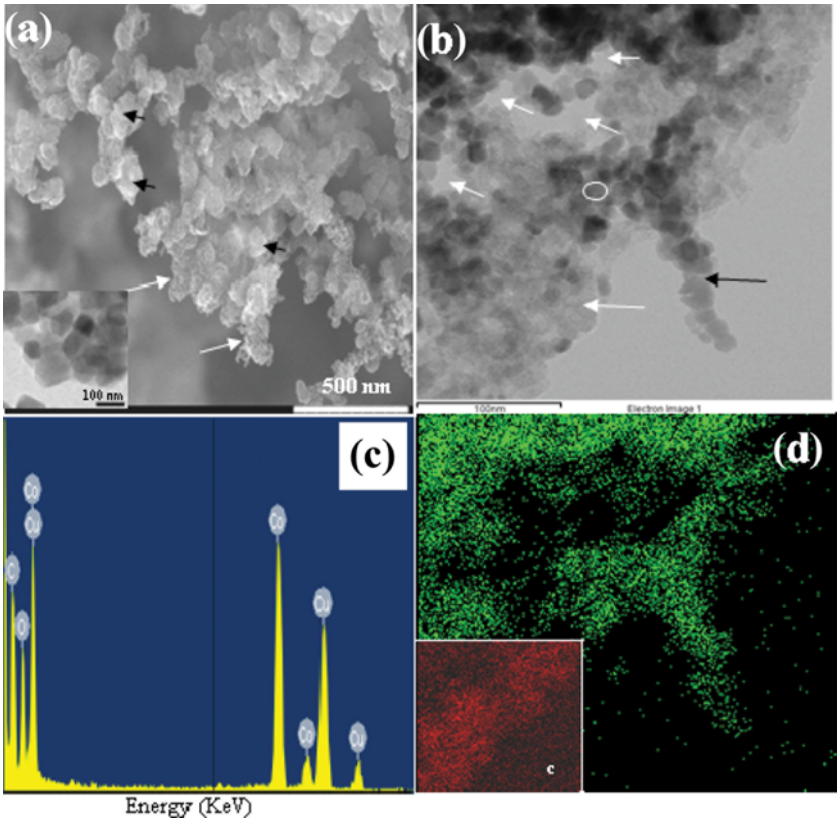

Fig. 2. (a) SEM image of the Co_3O_4/C composite. White arrows indicate the presence of a porous carbon network, and small black arrows indicate the Co_3O_4 nanoparticles embedded in the carbon network. The inset shows a TEM image of Co_3O_4 nanoparticles (sample C). (b) TEM image of CC composite; the small white arrows indicate the porous nature of the carbon, while the larger arrow indicates substantial arrangement of the amorphous carbon; the black arrow shows the agglomerated Co_3O_4 nanoparticles. (c) EDX spectrum of the CC composite. (d) Elemental mapping images of the cobalt (green) and carbon (red, inset of image (d)).

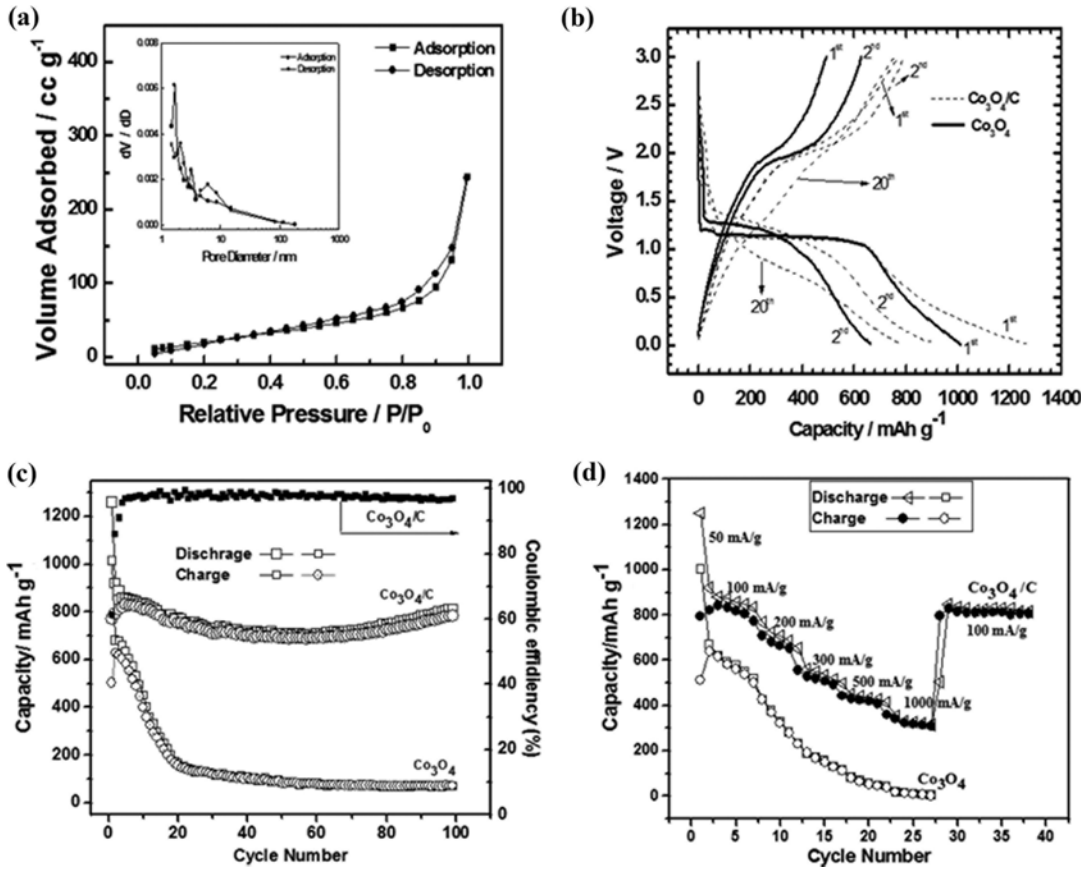

Fig. 3. (a) Nitrogen adsorption-desorption isotherm and corresponding pore size distribution curve (inset) of Co_3O_4/C sample. (b) Electrochemical screening of Co_3O_4 and Co_3O_4/C electrodes for lithium-ion secondary batteries at a current density of 50 mA g^{-1}. Charge/discharge voltage profiles of electrodes fabricated using Co_3O_4, Co_3O_4/C: (c) cycling performance for 100 cycles and (d) rate capability of Co_3O_4 and Co_3O_4/C electrodes at various current densities.

using TGA between 50 and 1,000 °C in air. The TGA curve of the Co_3O_4/C composite shows a gradual weight loss up to 1,000 °C. In comparison, the bare Co_3O_4 nanoparticles show little weight loss to 900 °C, and the Super-P carbon show substantial weight loss at much lower temperatures. Based on the thermal behavior observed, the weight ratio of the carbon in the composite was estimated to be 30 wt% (Fig. 1(b)).

After annealing, the precursor carbon nanoparticles were aggregated, leaving nano/mesopores that formed a porous carbon network with entrenched 50-100 nm Co_3O_4 nanoparticles (see Fig. 2(a) for sample CC). The inset of Fig. 2(a) shows a TEM image of the bare Co_3O_4 nanoparticles of sample C. Fig. 2(b) shows a TEM image of the composite CC, in which the meso/nanopores of the carbon network are indicated by the small white arrows. The larger arrow in Fig. 2(b) shows the carbon network obtained as a result of the self-aggregation of carbon particles during heat treatment. As shown, most of the Co_3O_4 nanoparticles were entrapped within the carbon network. This kind of carbonization of metal oxide particles should improve the composite conductivity and may provide a shielding layer against the $LiPF_6$ electrolyte during cycling. An EDX elemental data graph (shown in Fig. 2(c)) illustrates the presence of carbon within composite sample CC together with the presence of Co and O elements. Elemental mapping data shown in Fig. 2(d) and its inset image show the distribution of Co (green) and C (red) within sample CC.

Fig. 3(a) shows the absorption isotherms of the Co_3O_4/C sample, indicating the presence of mesopores (1-50 nm). The shapes of the hysteresis loops are type H3 in the relative pressure range from 0.4 to 1.0, which implies the formation of mesopores and nanopores [12]. The pore size distributions (inset of Fig. 3(a)) are uneven with distinct mesopores and nanopores ranging between 1-10 nm. These pores correspond to the voids between the accumulated carbon particles. The measured surface area for the composite was about 48 m^2 g^{-1}, which is high enough that it may improve the electrode performance by facilitating the active electrode/electrolyte interaction.

2. Application in Li-ion Rechargeable Batteries

Co_3O_4 nanoparticles and the Co_3O_4/C composite were tested as anode electrodes in Li-ion secondary batteries by using galvanostatic charge-discharge cycling at a current density of 50 mAg^{-1}. Fig. 3(b) shows the charge-discharge profiles of Co_3O_4 nanoparticles (1st, 2nd cycles) and the composite Co_3O_4/C (1st, 2nd and 20th) electrodes. The main voltage plateaued at 1.13 to 1.16 V in the discharge curves followed by a sloping curve, which is characteristic of Co_3O_4 electrodes [8,9,13]. The first discharge and charge capacities were 1,014 and 490 $mAhg^{-1}$ for Co_3O_4 and were 1,260 and 768 $mAhg^{-1}$ for composite Co_3O_4/C, respectively. Note that the nano-

structured arrangement of the Co_3O_4 particles provides an appreciable increase in the initial capacities compared to the theoretical capacities, i.e., 890 $mAhg^{-1}$ for bulk Co_3O_4 and about 300 $mAhg^{-1}$ for carbon materials [8,9]. The first coulombic efficiencies (61% for Co_3O_4/C and 49% for Co_3O_4 electrodes) are low, and this could be ascribed to irreversible Li^+ ion conversion reactions resulting in solid electrolyte interphase (SEI) formation [9,13].

Fig. 3(c) shows the cycle performance of the electrodes over 100 cycles. The Co_3O_4 electrode shows discharge capacity fading from the 2nd cycle up to 20th cycle before finally stabilizing at about 70 $mAhg^{-1}$. The large-volume expansion during Li^+ ion insertion led to abrupt agglomeration of nanoparticles that caused the rapid degradation in capacity [13]. Despite its initial low coulombic efficiency, the Co_3O_4/C electrode displays excellent cycling stability by delivering 780 $mAhg^{-1}$ with more than 99% coulombic efficiency over 100 cycles (Fig. 3(c)). The rate capabilities of the Co_3O_4 and Co_3O_4/C electrodes at different current densities ranging from 50 mAg^{-1} to 1,000 mAg^{-1} are shown in Fig. 3(d). The results reveal that the composite Co_3O_4/C shows excellent rate performance. Specifically, it has a good reversible capacity of 798 $mAhg^{-1}$ at a rate of 100 mAg^{-1}, which slowly decreases to 656 $mAhg^{-1}$ at 200 mAg^{-1} and 310 $mAhg^{-1}$ at 1,000 mAg^{-1}. Interestingly, the composite Co_3O_4/C electrode recovers its capacity even after cycling at different rates, providing 829 $mAhg^{-1}$ at 100 mAg^{-1}, which is almost equal to the reversible capacities delivered in the initial cycles. Furthermore, the Co_3O_4/C electrode maintains a steady cycle life, delivering 807 $mAhg^{-1}$ for the subsequent 10 cycles. In comparison, the Co_3O_4 electrode shows inferior rate capability performance due to the substandard electrochemical performance resulting from the randomly aggregated Co_3O_4 nanoparticles (as confirmed by inset image of Fig. 2(a)).

In this work, the composite electrode shows fairly good electrochemical performance. Specifically, it shows a very good reversible capacity of 480 mAh g^{-1} at 500 mA g^{-1}, which is better than that obtained used current carbon anode materials [14], Co_3O_4/CNT [3], Co_3O_4/carbon nanofiber [9,15]. The reversible capacity is comparable to that of graphene/Co_3O_4 composites [11,16]. The Co_3O_4/C composite shows highly reversible behavior and retains its specific capacity at a coulombic efficiency of >97% after being cycled at different rates. Furthermore, we compared the results obtained from different Co_3O_4/carbon composites reported in literature to the present results as shown in Table 1 [17-20]. The admirable anode performance of the composite Co_3O_4/C electrode in this work is attributed to the surface characteristics of the porous carbon network confined by highly crystalline Co_3O_4 nanoparticles. The resulting hybrid material provides a large active area exposed to electrochemical reactions and also prevents the aggregation of particles that can occur during prolonged cycling.

CONCLUSIONS

A highly reactive starting precursor material, $Co_2(CO)_8$, interacted with the carbon nanoparticles after sonication in a non-polar solvent. The subsequent low-temperature calcination treatment resulted in the formation of a hybrid material with Co_3O_4 nanoparticles that were confined in a meso/nanoporous carbon network. This resulting Co_3O_4/C composite was used as an electrode for rechargeable Li-ion batteries. As an anode in Li-ion batteries, the Co_3O_4/C composite showed excellent cycling stability with a very good rate capability, which was better than that of conventional carbon materials.

ACKNOWLEDGEMENTS

This research was supported by the Basic Science Research Program through the National Research Foundation of Korea (NRF) funded by the Ministry of Science, ICT & Future Planning (2014R1A5A1009799). This work was also supported by a grant from Kyung Hee University in 2014 (KHU-20140324) and a grant from Kyung Hee University in 2015 (KHU-20150516).

REFERENCES

1. R. F. Zhou, C. Z. Meng, F. Zhu, Q. Q. Li, C. H. Liu, S. S. Fan and K. L. Jiang, *Nanotechnology*, **21**, 345701 (2010).
2. C. T. Heish and J. Y. Lin, *ECS Transactions*, **13**, 73 (2008).
3. Y. Shan and L. Gao, *Chem. Lett.*, **33**, 1560 (2004).
4. T. H. Yoon and Y. J. Park, *Nanoscale Res. Lett.*, **7**, 1 (2012).
5. R. J. Wu, J. G. Wu, M. R. Yu, T. K. T. Sai and C. T. Yeh, *Sen. Lett.*, **6**, 848 (2008).
6. J. W. Lang, X. B. Yan and Q. J. Xue, *J. Power Sources*, **196**, 7841 (2011).
7. N. Venugopal and W.-S. Kim, *Korean J. Chem. Eng.*, **32**, 1918 (2015).
8. (a) Y. Shan and L. Gao, *Mat. Chem. Phy.*, **103**, 206 (2007).
   (b) B. J. Li, H. Q. Cao, J. Shao, G. Q. Li, M. Z. Qu and G. Yin, *Inorg. Chem.*, **50**, 1628 (2011).
9. W. L. Yao, J. L. Wang, J. Yang and G. D. Du, *J. Power Sources*, **176**, 369 (2008).
10. (a) Y. He, L. Huang, J. S. Cai, X. M. Zheng and S. G. Sun, *Electrochim. Acta*, **55**, 1140 (2010).

Table 1. Comparison of the performance of Co_3O_4/carbon nanocomposites as anode materials or lithium ion batteries

Active material	Current density mA g^{-1}	Reversible capacity mA h g^{-1}	Cycle life	References
CNT/Co_3O_4	200	823 After 60 cycles	96.8% Retention during 60 cycle	17
Carbon/Co_3O4	100	534 After 20 cycles	69.8% Retention during 20 cycles	18
Carbon/Co_3O_4	50	779 After 50 cycles	86.1% Retention during 50 cycles	19
Graphene/Co_3O_4	100	1003 After 50 cycles	90.6% Retention during 50 cycles	20
Graphene/Co_3O_4	50	935 After 30 cycles	86.3% Retention during 30 cycles	13
Graphene/Co_3O_4	100	840 After 40 cycles	83.5% Retention during 40 cycles	13
Co_3O_4/C	100	780 After 100 cycles	99% Coulombic efficiency over 100 cycles	In this work

(b) K. H. Park, D. Lee, J. Kim, J. Song, Y. M. Lee, H.-T. Kim and J.-K. Park, *Nano Lett.*, **14**, 4306 (2014).
11. N. Du, H. Zhang, B. Chen, J. B. Wu, X. Y. Ma, Z. H. Liu, Y. Q. Zhang, D. Yang, X. H. Huang and J. P. Tu, *Adv. Mater.*, **19**, 4505 (2007).
12. K. S. W. Sing, *Pure Appl. Chem.*, **54**, 2201 (1982).
13. Z. S. Wu, W. C. Ren, L. Wen, L. B. Gao, J. P. Zhao, Z. P. Chen, G. M. Zhou, F. Li and H. M. Cheng, *ACS Nano*, **4**, 3187 (2010).
14. T. Zheng and J. R. Dahn, *Applications of carbon in lithium-ion batteries, in Carbon Material of Advanced Technology*, Pergamon Press, Oxford, UK (1999).
15. W. L. Yao, J. Yang, J. L. Wang and L. A. Tao, *Electrochim. Acta*, **53**, 7326 (2008).
16. H. Kim, D. H. Seo, S. W. Kim, J. Kim and K. Kang, *Carbon*, **49**, 326 (2011).
17. L. Zhuo, Y. Wu, J. Ming, L. Wang, Y. Yu, X. Zhang and F. Zhao, *J. Mater. Chem. A*, **1**, 1141 (2013).
18. P. Zhang, Z. P. Guo, Y. Huang, D. Jia and H. K. Liu, *J. Power. Sources*, **196**, 6987 (2011).
19. F. Hao, Z. Zhang and L. Yin, *ACS Appl. Mater. Interfaces*, **5**, 8337 (2013).
20. B. G. Choi, S. J. Chang, Y. B. Lee, J. S. Bae, H. J. Kim and Y. S. Huh, *Nanoscale*, **4**, 5924 (2012).